Flow Reversal and Intermittency of a Turbulent Jet

L. P. Chua* and R. A. Antonia†
University of Newcastle, New South Wales, Australia

Using data obtained with a combination of an X-probe and a single cold wire, an attempt is made to quantify the importance of flow reversal in the intermittent region of a turbulent circular jet discharged into still air and its influence on both conventional and conditional velocity fluctuations. It is found that flow reversal coincides with high probability with nonturbulent periods but occurs for only a small fraction of the time for which the flow is nonturbulent. This result is consistent with the observation that conventional and zone-averaged Reynolds stresses and heat fluxes are essentially unaffected by flow reversal.

Nomenclature

d = nozzle diameter
f = frequency
I = intermittency function defined by Eq. (2)
p_θ = probability density function of θ, where $\int_{-\infty}^{\infty} p_\theta(\alpha)\, d\alpha = 1$
q = fluctuating quantity, e.g., u, v, or θ, such that $\bar{q} \equiv 0$
r = radial distance from jet centerline
R = flow reversal function defined by Eq. (1)
R_0 = half-velocity radius where $\bar{U} = U_0/2$
t_f = total record duration
TH_1, TH_2 = dimensionless thresholds used for intermittency detection
TH_R = dimensionless threshold used for flow reversal detection
u = axial velocity fluctuation in x direction
$\bar{U}$ = local mean velocity in x direction
U_0 = maximum local mean velocity
v = velocity fluctuation in the radial direction
$\bar{V}$ = radial mean velocity
x = axial distance
β = velocity vector cone angle
η = dimensionless coordinate, $\eta \equiv r/R_0$
θ = temperature fluctuation
θ_1 = noncontaminated temperature
$\bar{\Theta}$ = mean local temperature
Θ_0 = maximum local mean temperature
ρ = correlation coefficient between R and I; $\rho \equiv \overline{(R-\bar{R})(I-\bar{I})}/\overline{(R-\bar{R})^2}^{\frac{1}{2}}\,\overline{(I-\bar{I})^2}^{\frac{1}{2}}$
τ = duration for which θ data are ignored before and after a signal patch that satisfies $\theta > TH_R\bar{\Theta}$
ϕ_θ = spectral density function of θ, where $\int_0^\infty \phi_\theta(f)\, df = 1$

Subscripts and Superscripts

0 = value on axis of symmetry
1 = refers to noncontaminated data
j = value at nozzle exit
NR = refers to zone with no flow reversal
NT = refers to nonturbulent zone
R = refers to zone with flow reversal
T = refers to turbulent zone
prime = root mean square value, i.e., $()' = \overline{()^2}^{\frac{1}{2}}$
overbar = time average taken over total duration t_f for unsubscripted quantities, e.g., $\bar{q} = t_f^{-1}\int_0^{t_f} q\, dt$, or over a duration occupied by the zone of interest in the case of subscripted quantities, e.g., $\bar{q}_R$, $\bar{q}_T$ defined by Eqs. (3) and (5), respectively

Introduction

HOT-WIRE measurements in the outer part of turbulent jets that discharge into "still" air or "stagnant" surroundings are prone to errors resulting from high local turbulence intensities and the possibility of flow reversal. These difficulties disappear when an external stream is used, as was done for example by Bradbury[1] in the case of a plane jet or by Antonia et al.[2] in the case of a circular jet, but the characteristics of coflowing jets, even when the velocity of the secondary stream is small compared with that of the main jet, may differ appreciably from those of jets issuing into "still" air. Techniques available for the measurement of velocity fluctuations in flows with relatively high turbulence levels include laser Doppler anemometry,[3] the flying hot wire[4,5] and pulsed-wire anemometry.[6,7] However, when the interest has focused on the simultaneous determination of velocity and temperature fluctuations, measurements have been made with a cold-wire/X-probe combination. It has recently[8,9] been shown that a 120-deg X-proble yields values for the Reynolds shear stress near a rough wall in good agreement with those obtained with a flying X-probe. However, most, if not all, measurements that have been published[10,11] were made with a standard 90-deg X-probe. For this reason, the standard X-probe configuration has been used in the present investigation. Antonia et al.[12] identified flow reversal by using a cold wire placed parallel to and at a small distance upstream of a hot wire to detect the thermal wake of the hot wire, the two-wire arrangement being operated in an unheated circular jet. A similar arrangement was used by Goldschmidt et al.[13] in a plane jet.

In the present investigation, flow reversal is detected by placing a cold-wire/X-probe arrangement in a heated circular jet. The cold wire is perpendicular to the plane of the X-probe and at a small distance upstream from the point of intersection of the X-wires, so as to detect the thermal wake of the hot wires.

It was observed in Ref. 12 that flow reversal usually occurs in the nonturbulent part of the flow. It was also found that higher-order moments of u, with the averaging taken over a duration where no flow reversal occurred, did not differ appreciably from conventionally averaged moments. Although a few flow reversal statistics were presented in Ref. 12,

Received Aug. 15, 1988; revision received Nov. 14, 1988.

*Postgraduate Student, Department of Mechanical Engineering.
†Professor, Department of Mechanical Engineering.

the relationship between intermittency and flow reversal was not considered systematically. The aim of this paper is to quantify the importance of flow reversal in the intermittent region of a turbulent circular jet and its influence on the measurement of both conventional and conditional statistics of velocity fluctuations. Estimates are made of the fractions of time for which flow reversal occurs and for which the flow is turbulent and to determine the extent of the correlation between flow reversal and the turbulent region of the flow. Statistics of the velocity fluctuations u, v, the temperature fluctuation θ, and the products uv, $v\theta$ are obtained for several flow regions or zones: turbulent, nonturbulent, those for which flow reversal occurs, and those that are free of flow reversal.

Experimental Details and Conditions

The experimental facility, described in Chua and Antonia,[14] comprises a variable speed centrifugal blower that supplies air to an axisymmetric nozzle with a 10 : 1 contraction ratio. The jet is heated with 1-kW electrical coil elements distributed across the duct. The exit diameter d of the nozzle is 25.4 mm.

The velocity fluctuations u, v and temperature fluctuation θ were measured with an X-probe/cold-wire arrangement sketched in Fig. 1a. The X-probe hot wires (5-μm diameter Pt-10% Rh, length $\approx$ 1.1 mm) with an included angle of approximately 90 deg were separated by about 0.7 mm. A 90-deg X-probe has been preferred in this study because this is the configuration that has been used by other authors.[10,11] It has been shown[15] that the 90-deg X-probe can underestimate the rms values of the vector cone angle and the lateral velocity fluctuation.

The wires were mounted in the (x, r) plane (see Fig. 1b for definition of coordinates) and operated in an overheat of 0.5 in DISA 55M10 constant temperature circuits. The cold-wire (0.63-μm diameter Pt-10% Rh) was placed about 0.6 mm upstream of the center of the X-probe perpendicular to the X-probe plane. The length of the cold wire was approximately equal to 1.8 mm, which was long enough to prevent any interference of the wakes from the unetched part of the cold wire with the hot wires. The cold wire was operated with constant current circuit. The current used was 0.1 mA, and the resulting sensitivity of the wire to velocity fluctuation was sufficiently small [$\approx 2.8 \times 10^{-3}$ K(m/s)$^{-1}$] to be ignored; e.g., the resulting error in the maximum value of u' would be less than 0.1%. Using the pulsed-wire technique described in Antonia et al.,[16] the frequency response of the 0.63-μm wire was estimated to be about 3.5 kHz at a velocity of 5 ms^{-1}.

The X-probe was calibrated for the velocity and yaw in the potential core of the cold jet. Yaw angles in the range -36 to 36 deg were used in 9-deg steps. For each yaw angle, the probe was calibrated over a range of velocities present at the measurement station. Details of this full velocity vs yaw angle calibration approach, which allows instantaneous velocity components to be determined without the need to assume specific wire cooling laws, are given in Browne et al.[17] This approach, which is somewhat similar to the lookup table approach of Lueptow et al.,[18] is an improvement over the constant effective angle approach, particularly for the present flow, where the turbulence intensity is high (e.g., $u'/U_0 \approx 0.22$ at $r = 0$). The temperature sensitivity ($\approx 1.69 \times 10^{-3}$ K^{-1}) of the cold wire was determined with the wire placed at the nozzle exit using a 10-Ω platinum resistance thermometer operated in a Leeds and Northrup 8078 bridge capable of resolving 0.01 K. The jet velocity was measured with a pitot tube connected to a Furness micromanometer with a least count of 0.01 mm water. A data logger consisting of a data acquisition system (HP3497A) and a desktop computer (HP85) were used during calibration.

Wire voltages were digitized, after applying suitable offsets and amplifications, on a PDP 11/34 computer at a sampling frequency of 2500 Hz. Before digitizing, the signals were low-pass filtered at a cutoff frequency of 1250 Hz. The record

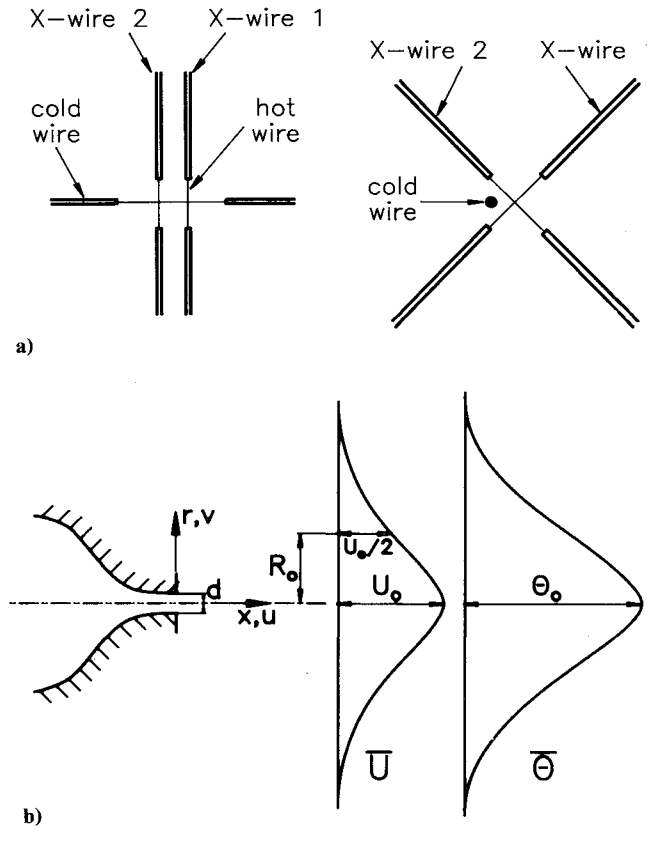

Fig. 1 a) Configuration of the cold-wire/X-probe arrangement; b) definition sketch.

duration was about 41 s, which is sufficient to ensure convergence of the data. For example, the final values of $\overline{uv}$ and $\overline{v\theta}$ averaged within $\pm 5\%$ and $\pm 6\%$, respectively, for durations typically equal to 80% of the total record duration. The digital data were stored on magnetic tape for processing on a VAX 8550 computer. The digitized hot-wire voltages were converted to velocities, correcting the effect of air temperature changes on the heat transfer from the wires. The correction involved multiplying the wire voltages[19] by $(T_w - T_a)/(T_w - T_f)$, where T_w is the wire temperature, T_a the ambient temperature and T_f the instantaneous air temperature.

All measurements were made at a streamwise distance of $15d$, with a jet exit velocity U_j of 11 m/s and a jet exit temperature, relative to ambient, of 25 K. The Reynolds number based on d is equal to 17,700. At the nozzle exit, the boundary layer is laminar, but the mixing layer is fully turbulent at $x/d \approx 2.4$. A detailed description of the jet initial conditions, including schlieren photographs of the near-jet region, is given in Chua and Antonia.[14]

Definitions

To quantify the importance of flow reversal and its likely relationship to intermittency, a flow reversal function $R(t)$ is defined in a manner analogous to the definition of the intermittency function $I(t)$,[20,21] viz. The functions $R(t)$ and $I(t)$ are defined as follows:

$$R(t)\begin{cases} = 1 & \text{when flow reversal occurs} \\ = 0 & \text{where there is no flow reversal} \end{cases} \quad (1)$$

$$I(t)\begin{cases} = 1 & \text{when the flow is turbulent} \\ = 0 & \text{when it is nonturbulent} \end{cases} \quad (2)$$

The average values $\bar{R}$ and $\bar{I}$ represent the flow reversal factor and the intermittency factor, respectively. Variable $\bar{R}$ represents the fraction of time for which reversal occurs, while $\bar{I}$ is

the fraction of time for which the flow is turbulent. The definition of the on/off functions $R(t)$ and $I(t)$ permits averages of any quantity q in a particular flow zone, e.g.,

$$\bar{q}_R = \frac{1}{\bar{R}t_f}\int_0^{t_f} R(t)q(t)\,dt \tag{3}$$

$$\bar{q}_{NR} = \frac{1}{(1-\bar{R})t_f}\int_0^{t_f} [1-R(t)]q(t)\,dt \tag{4}$$

$$\bar{q}_T = \frac{1}{\bar{I}t_f}\int_0^{t_f} I(t)q(t)\,dt \tag{5}$$

$$\bar{q}_{NT} = \frac{1}{(1-\bar{I})t_f}\int_0^{t_f} [1-I(t)]q(t)\,dt \tag{6}$$

where the subscripts R, NR denote zones with flow reversal and no flow reversal, respectively, while T and NT denote turbulent and nonturbulent flow regions, respectively. In the present context, q can represent any of the following quantities: u, v, θ, the velocity vector angle β, or the products uw and $v\theta$. Zone averages are related to conventional averages in the usual way, viz.,

$$\bar{q} = \bar{R}\bar{q}_R + (1-\bar{R})\bar{q}_{NR} \tag{7}$$

$$\bar{q} = \bar{I}\bar{q}_T + (1-\bar{I})\bar{q}_{NT} \tag{8}$$

and

$$\overline{q^2} = \bar{R}\overline{(q-\bar{q}_R)^2_R} + (1-\bar{R})\overline{(q-\bar{q}_{NR})^2_{NR}} + \bar{R}(1-\bar{R})(\bar{q}_R+\bar{q}_{NR})^2 \tag{9}$$

$$\overline{q^2} = \bar{I}\overline{(q-\bar{q}_T)^2_T} + (1-\bar{I})\overline{(q-\bar{q}_{NT})^2_{NT}} + \bar{I}(1-\bar{I})(\bar{q}_T-\bar{q}_{NT})^2 \tag{10}$$

Statistics of q in any particular zone will always be taken with respect to the average of q in that zone. For ease of writing, a prime will denote the rms of a zone-averaged quantity, e.g., $q'_R = (q-\bar{q}_R)^{2\,1/2}_R$ and $q'_{NR} = (q-\bar{q}_{NR})^{2\,1/2}_{NR}$.

The products RI and $R(1-I)$ have the following useful properties:

$$RI = \begin{cases} 1 & \text{when } R=1 \text{ and } I=1 \\ 0 & \text{otherwise} \end{cases} \tag{11}$$

$$R(1-I) = \begin{cases} 1 & \text{when } R=1 \text{ and } I=0 \\ 0 & \text{otherwise} \end{cases} \tag{12}$$

The average $\overline{RI}$ is the fraction of total time for which the flow is turbulent with the simultaneous occurrence of flow reversal. The average $\overline{R(1-I)}$ is the fraction of total time for which the flow is nonturbulent and flow reversal occurs simultaneously.

Indicators of Flow Reversal

Observations of the temperature fluctuation θ recorded in the heated jet with the X-wires operating, show that the level of contamination increases as the radial distance increases in similar fashion to the temperature signals shown in Ref. 12. The contamination, indicated by arrows in Fig. 2a, is due to the thermal wakes from the X-probe wires. When the X-probe is switched off, the temperature fluctuation θ_1 (Fig. 2b) shows no contamination. The comparison between θ'/Θ_0 and θ'_1/Θ_0 (Fig. 3) provides an indication of the intensity of temperature contamination. The difference between θ'/Θ_0 and θ'_1/Θ_0 is first noticeable at $\eta \approx 1.0$, where θ' exceeds θ'_1 by about 9%. The difference increases rapidly for $\eta > 1$. To check that the

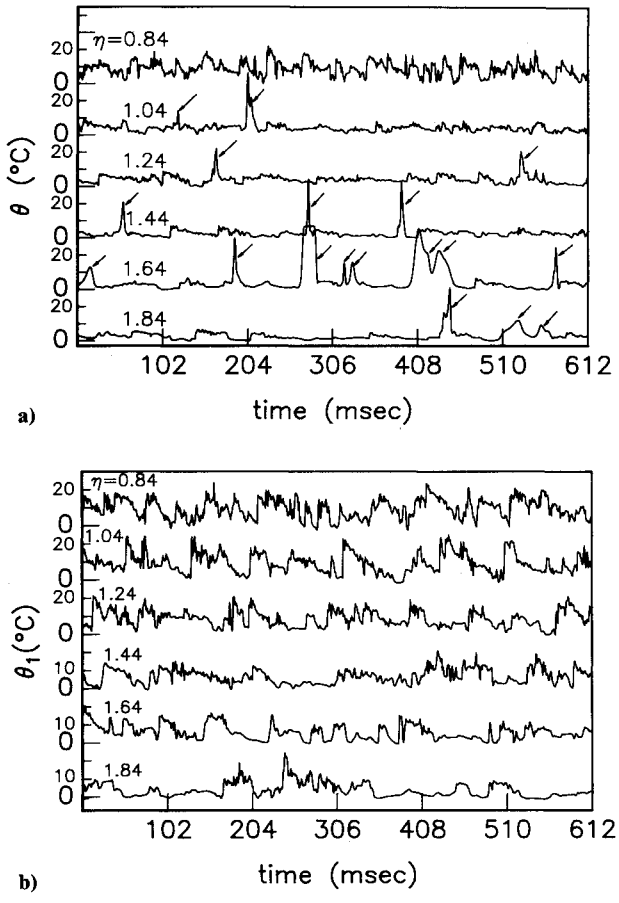

Fig. 2 a) Temperature signals (θ) when the X-probe is operating; b) temperature signals (θ_1) when the X-probe is switched off at $x/d = 15$. The signals are recorded at $x/d = 15$ for several values of η.

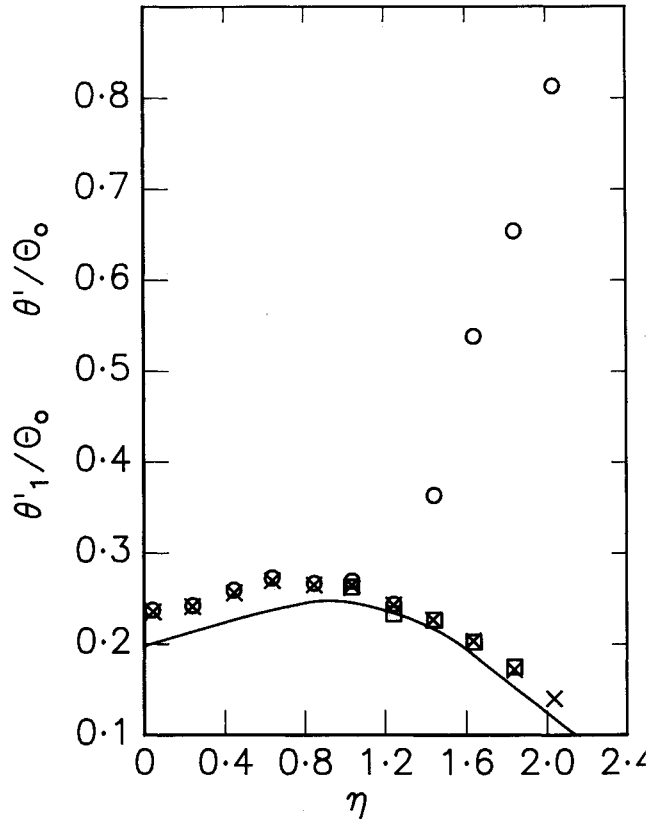

Fig. 3 Variation of rms temperature across the jet: ○, θ'/Θ_0; □, θ'_{NR}/Θ'_0; ×, θ'_1/Θ_0; ——, θ'_1/Θ_0, Chevray and Tutu.[11]

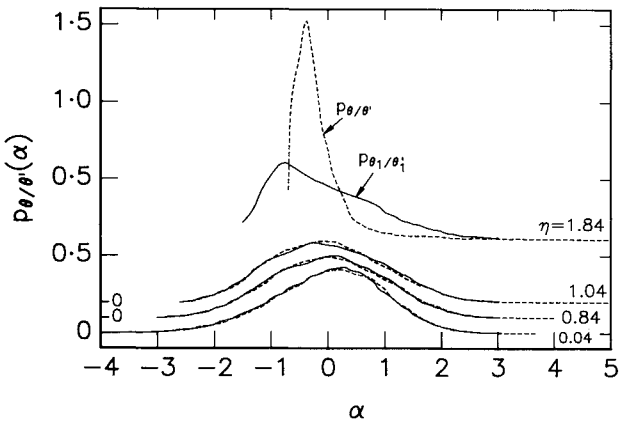

Fig. 4 Probability density functions of contaminated (θ) and noncontaminated (θ_1) temperature fluctuations at four values of η: $\eta = 0.04$; 0.84; 1.04; 1.84. —, $p_{\theta 1}$; — — —, p_θ.

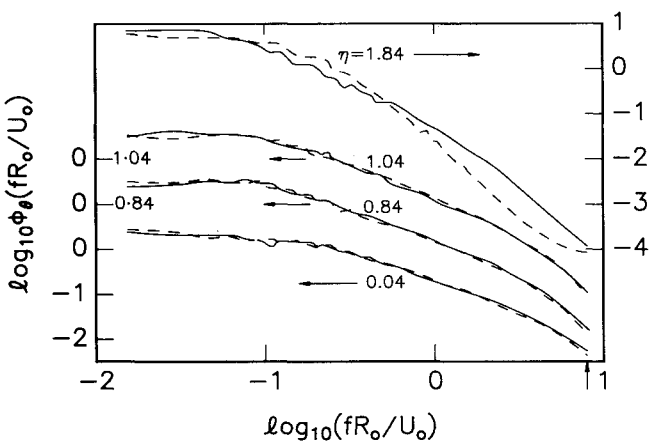

Fig. 5 Spectra of contaminated (θ) and noncontaminated (θ_1) temperature fluctuations at four values of η. The vertical arrow on the abscissa corresponds to the cutoff frequency of the low-pass filter. —, $\phi_{\theta 1}$; — — —, ϕ_θ.

distribution of θ_1' was not affected by the presence of the X-probe, the rms temperature was remeasured after the X-probe was removed. No difference could be detected between the two distributions. The present distribution of θ_1'/Θ_0 is in reasonable agreement with that of Chevray and Tutu.[11]

While the rms temperature is one indicator of the degree of contamination, other indicators are the probability density function (*pdf*) p_θ and spectral density function ϕ_θ. The evolution, with respect to η, of the *pdf*s of θ and θ_1 is shown in Fig. 4. The p_θ and $p_{\theta 1}$ are nearly identical for $\eta = 0.04$ and 0.84. Figure 4 shows that p_θ has a long positive tail, implying that the contamination resulting from the thermal wakes of the hot wires first appears at $\eta \approx 1.0$. This is consistent with previous inferences from Fig. 3. The comparison between p_θ and $p_{\theta 1}$ at $\eta = 1.84$ in Fig. 4, apart from indicating the level of contamination, suggests that the shape of $p_{\theta 1}$ can provide useful guidance when correcting the θ signal.

For $\eta \leq 1$, Fig. 5 shows that there is practically no difference between ϕ_θ and $\phi_{\theta 1}$. At $\eta = 1.84$, there is an attenuation of the high frequency part of $\phi_{\theta 1}$ relative to ϕ_θ, but the difference between ϕ_θ and $\phi_{\theta 1}$ is nowhere near as pronounced as the difference between p_θ and $p_{\theta 1}$ in Fig. 4 for the same η position. This implies that the shape of the spectrum is not as sensitive an indicator of flow reversal as the shape of the *pdf*.

Formation of Flow Reversal and Intermittency Functions

The contamination of the temperature signal by the thermal wakes of the X-wires is generally characterized by the appearance of relatively high-amplitude spikes (the term used in Ref. 12). A few spikes can be seen in the temperature trace at the bottom of Fig. 6. A possible method of removing the contamination would consist of ignoring the data for which θ exceeds $TH_R\bar{\Theta}$, where TH_R is a threshold parameter. Since a relatively large value of TH_R was needed to avoid eliminating good data, an equivalent time duration τ of data points were ignored just before and after a patch of signal that satisfied the criterion $\theta > TH_R\Theta$. At best, this procedure is a compromise, since good data may be discarded in the process.

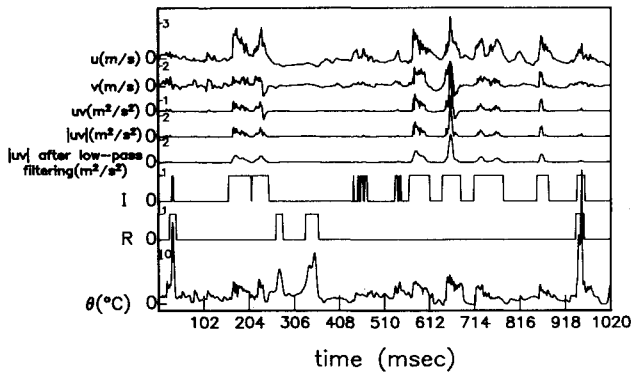

Fig. 6 Velocity and temperature signals used to form the flow reversal and intermittency functions; $\eta = 1.84$. Signals are shown for a duration of 1 s.

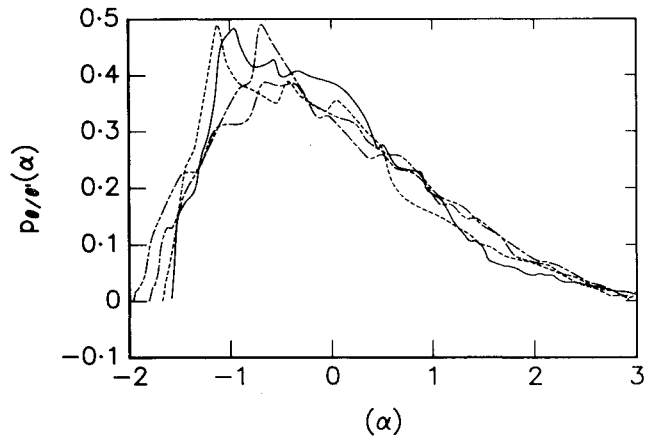

Fig. 7 Comparison between the *pdf* of the noncontaminated temperature θ_1 and that of the temperature signal corrected for flow reversal. The corrected *pdf* is shown for different choices of detection parameters. —, $p_{\theta 1}$; — — —, $TH_R = 0.81$, $\tau U_0/R_0 = 0.63$; — - —, $TH_R = 0.88$, $\tau U_0/R_0 = 0.63$; — - - —, $TH_R = 0.94$, $\tau U_0/R_0 = 1.01$.

The period of time for which R (see Fig. 6) has been set equal to unity includes the data points that satisfy $\theta > TH_R\bar{\Theta}$ as well as the previously mentioned 2τ data points. To optimize TH_R and τ, several choices were made for these parameters (typically for the example in Fig. 6, $0.81 < TH_R < 0.94$ and $0.31 < \tau U_0/R_0 < 1.01$). The visual comparison of computer plots of R and θ provides a useful indication of the appropriateness of these parameters. To test the selection of the parameters TH_R and τ, a comparison was made between θ_{NR}', the rms of the temperature signal following the removal of the contaminated parts, with θ_1', the rms of the uncontaminated signal. The *pdf* of θ_{NR} was also compared with the *pdf* of θ_1. At $\eta = 1.84$ (the largest value of η considered here and hence the location at which the contamination is largest), the selection $TH_R = 0.81$ and $\tau U_0/R_0 = 0.63$ yielded a value of 0.179 for θ_{NR}'/Θ_0 compared with 0.174 for θ_1'/Θ_0. Figure 7 indicates that for these values of TH_R and τ, there is satisfactory agreement between the *pdf* of θ_{NR} and *pdf* of θ_1 at $\eta = 1.84$. Note that TH_R and τ were adjusted at each value of η to achieve the best agreement between rms values

Table 1

η	$\bar{R}$	$\bar{I}$	ρ	$\overline{RI}$	$\overline{R(1-I)}$	$\overline{RI}/\bar{I}$	$\overline{R(1-I)}/(1-\bar{I})$
1.04	0.001	0.857	0.003	0.001	0.000	0.001	0.001
1.24	0.003	0.738	−0.020	0.002	0.001	0.003	0.005
1.44	0.029	0.577	−0.055	0.012	0.017	0.021	0.040
1.64	0.087	0.418	−0.074	0.026	0.061	0.062	0.104
1.84	0.148	0.245	−0.064	0.026	0.121	0.107	0.161

(see Fig. 3) and probability density functions of θ_{NR} and θ_1.

Initially, an attempt was made to use θ_1 to generate $I(t)$ in a manner similar to that followed by Antonia et al.[2] However, this method had two drawbacks in the present case. First, the ambient temperature baseline of the temperature signal is not as steady as in the experiment of Antonia et al.,[2] where the coflowing stream provides a more favorable environment than the laboratory "still" air. Second, it was important to generate $I(t)$ simultaneously with $R(t)$ in order to obtain the required joint statistics between $R(t)$ and $I(t)$.

To form $I(t)$, the signal uv (Fig. 6) was preferred to either u or v, which have fluctuations of significant amplitude in the nonturbulent zones of the flow. The procedure included the following steps:

1) Only the absolute value of uv was used. This simplifies the computer detection scheme since only positive data need to be considered.

2) The $|uv|$ signal was then low-pass filtered to remove the high-frequency noise and increase the amplitude of the low-frequency components (see Fig. 6). The filter cutoff frequency, $f_c R_0/U_0 = 0.51$, was selected so that it is neither too high to retain the unnecessary high-frequency components nor too low to cause phase distortion of the filtered signals.

To generate $I(t)$, a window of duration τ_w ($\tau_w U_0/R_0 = 0.94$) is moved through the data point by point, and the mean and rms values of the data points within the window are calculated. When the criteria $|\overline{uv}| > TH_1|\overline{uv}|_{t_f}$ or $|uv|' > TH_2|uv|'_{t_f}$ are satisfied, the point at the center of the window is ascribed to a turbulent zone. The choices of TH_1 and TH_2 are based on the visual inspection of the on/off signal generated for $\bar{I}$. In general, smaller values of TH_1 and TH_2 result in larger values of $\bar{I}$. The resulting $I(t)$ signal is shown in Fig. 6.

Results and Discussion

Average values of R and I are shown in Table 1 for a region of the jet, $1 \lesssim \eta \lesssim 1.8$, where flow reversal is present. Also shown in the table is the magnitude of the correlation coefficient ρ between R and I as well as the values of $\overline{RI}$ and $\overline{R(1-I)}$. The flow reversal factor $\bar{R}$ increased slowly with η, but its magnitude remained small, with a maximum of about 0.15 at $\eta = 1.84$. The magnitude of the intermittency factor $\bar{I}$ and its decrease with η is in good agreement with the results of Chevray and Tutu.[11] The correlation coefficient ρ is generally small, its negative values suggest that, on average, I is unity when R is zero and vice versa. The fact that ρ is not quite zero reflects the possibility, confirmed by Fig. 6, that there are periods where $R(t)$ and $I(t)$ are both equal to unity. Comparison of the values $\bar{R}$, $\overline{RI}$, and $\overline{R(1-I)}$ in Table 1 indicates that, for $\eta \geq 1.44$, there is a greater probability that reversal will occur in the nonturbulent flow than in the turbulent flow. The reason is that the magnitude of the correlation $\overline{R(1-I)} = \bar{R} - \overline{RI}$ is nearly equal to $\bar{R}$, since $\overline{RI}$ is small. For $\eta \leq 1.24$, $\overline{RI}$ is larger than $\overline{R(1-I)}$, it means that in a flow region where $\bar{I}$ is almost unity and $\bar{R}$ is nearly zero, the probability of flow reversal is larger in a turbulent zone than in a nonturbulent zone.

The terms on the right side of Eq. (9) were evaluated for $q \equiv u$ and $q \equiv v$ and compared with the left side, viz. $\overline{q^2}$. The comparison was good in both cases, providing a useful consistency check of the data. The first and third terms on the right side of Eq. (9) were quite small (of the order of 10^{-2} and 10^{-3}, respectively, for $q \equiv u$) compared with the second term, so that a reasonable approximation to Eq. (9) is given by

$$\overline{q^2} = (1 - \bar{R})\overline{q^2_{NR}} \tag{13}$$

Distributions of q' and q'_{NR} are shown in Fig. 8 for $q \equiv u$, v, and β. In view of Eq. (13) and the relatively small magnitude of $\bar{R}$, it is not surprising that Fig. 8 shows a nearly one-to-one correspondence between averages in zones with no flow reversal and conventional averages. Similarly, there is nearly perfect agreement between conventional and zone averages of the products uv and $v\theta$, as shown in Fig. 9.

A reasonable explanation can be proposed for the predominance of flow reversal in nonturbulent zones. It has been shown[3,22] that an important feature of the self-preserving region of the circular jet is the existence of a relatively coherent large-scale motion. One expects this turbulent motion with vorticity on a scale comparable to the half-radius to convect in the x direction with a velocity comparable to U_0. When fixed sensors such as the present X-probe/cold wire

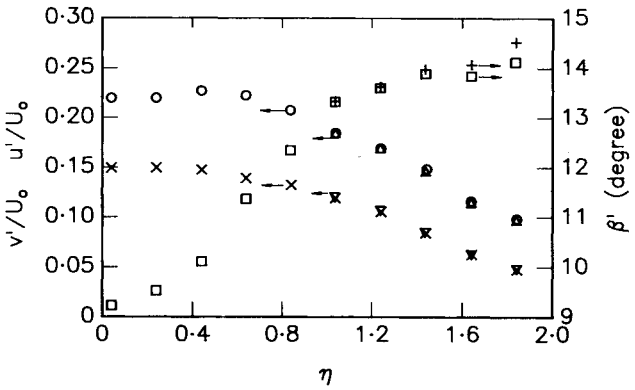

Fig. 8 Distributions of conventional and zone rms averages of velocity fluctuations and velocity vector cone angle fluctuations u'/U_0, v'/U_0 and β. ○, u'/U_0; Δ, u_{NR}/U_0; ×, v'/U_0; ∇, v'_{NR}/U_0; □, β' (deg) +, β'_{NR} (deg).

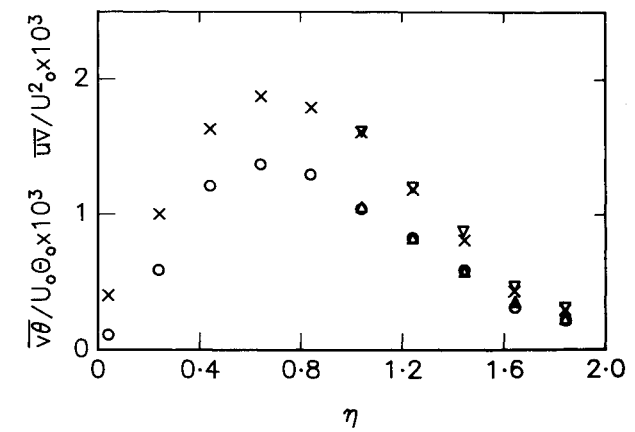

Fig. 9 Distributions of conventional and zone averages of the products uv and $v\theta$. ○, $\overline{(uv)}/U_0^2$; Δ, $\overline{(uv)}_{NR}/U_0^2$; ×, $\overline{(v\theta)}/U_0\Theta_0$; ∇, $\overline{(v\theta)}_{NR}/U_0\Theta_0$.

combination detect this motion, the resulting signals should exhibit turbulent characteristics and be nearly free of flow reversal since the large-scale motion, even when detected at relatively large η, has significant momentum in the positive x direction. By contrast, when the sensors detect a nonturbulent flow region, it is possible that this region contains fluid with a velocity in the negative x direction. This latter irrotational motion is induced by the vortical large-scale motion. The previous explanation does not exclude the possibility of reversal during turbulent regions: the turbulent/nonturbulent interface is expected to be convoluted and significantly three-dimensional so that there may be relatively narrow regions of turbulent fluid with only a small velocity in the negative x direction.

It has been mentioned in Ref. 12 that spikes usually occur in nonturbulent regions: consequently, they have a nearly symmetrical shape and are devoid of random fluctuations. When they occur in turbulent regions they are usually of shorter duration and have a higher frequency content than in the nonturbulent parts. A similar inference can be drawn by observing the θ trace (Fig. 6) in conjunction with the flow reversal and intermittency functions.

The last two columns in Table 1 give an indication as to why flow reversal has no apparent influence on either turbulent or nonturbulent zone averages. When the flow is turbulent, the fraction of time in which reversal occurs is small, as reflected by the ratio $\overline{RI}/\bar{I}$. Similarly, when the flow is nonturbulent, the fraction of time that corresponds to reversal is small, as reflected by the ratio $\overline{R(1-I)}/(I-\bar{I})$. Although $\overline{R(1-I)}/(1-\bar{I})$ is generally larger than $\overline{RI}/\bar{I}$, the probability of the occurrence of flow reversal in nonturbulent zones is not sufficient to affect nonturbulent zone averages adversely.

Conclusions

Flow reversal occurs only for a small fraction of the time in either turbulent or nonturbulent zones, thus corroborating the result that the removal of flow reversal zones does not change conventional or zone-averaged statistics significantly. In this context, published Reynolds shear stress and heat flux distributions should not require correction because of flow reversal in the outer part of the jet. However, the limitations of measurements made with 90-deg X-probes in a region of high turbulence intensity should be kept in mind.

Flow reversal occurs considerably more often when the flow is nonturbulent, a result that is most likely due to the irrotational motion induced by the large-scale vortical motion. The possibility that short periods of flow reversal can occur in turbulent zones is confirmed.

Acknowledgment

The support of the Australian Research Council is gratefully acknowledged.

References

[1]Bradbury, L. J. S., "The Structure of Self-Preserving Turbulent Plane Jet," *Journal of Fluid Mechanics*, Vol. 23, Sept. 1965, pp. 31–64.

[2]Antonia, R. A., Prabhu, A., and Stephenson, S. E., "Conditionally Sampled Measurements in a Heated Turbulent Jet," *Journal of Fluid Mechanics*, Vol. 72, Dec. 1975, pp. 455–480.

[3]Kumori, S. and Ueda, H., "The Large-Scale Coherent Structure in the Intermittent Region of the Self-Preserving Round Free Jet," *Journal of Fluid Mechanics*, Vol. 152, March 1985, pp. 337–359.

[4]Watmuff, J. H., Perry, A. E., and Chong, M. S., "A Flying Hot-Wire System," *Experiments in Fluids*, Vol. 1, 1983, pp. 63–71.

[5]Thompson, B. E. and Whitelaw, J. H., "Flying Hot-Wire Anemometry," *Experiments in Fluids*, Vol. 2, 1984, pp. 47–55.

[6]Bradbury, L. J. S. and Castro, I. P., "A Pulsed-Wire Technique for Velocity Measurements in Highly Turbulent Flows," *Journal of Fluid Mechanics*, Vol. 49, Oct. 1971, pp. 657–691.

[7]Jaroch, M., "Development and Testing of Pulsed-Wire Probes for Measuring Fluctuating Quantities in Highly Turbulent Flows," *Experiments in Fluids*, Vol. 3, 1985, pp. 315–322.

[8]Perry, A. E., Lim, K. L., and Henbest, S. M., "An Experimental Study of the Turbulence Structure in Smooth- and Rough-Wall Boundary Layers," *Journal of Fluid Mechanics*, Vol. 177, April 1987, pp. 437–466.

[9]Acharya, M. and Escudier, M. P., "Turbulent Flow Over Mesh Roughness," *Turbulent Shear Flows V*, edited by F. Durst, B. E. Launder, J. L. Lumley, F. W. Schmidt, and J. H. Whitelaw, Springer-Verlag, Berlin, 1987, pp. 176–185.

[10]Wygnanski, I. and Fiedler, H., "Some Measurements in the Self-Preserving Jet," *Journal of Fluid Mechanics*, Vol. 38, Sept. 1969, pp. 577–612.

[11]Chevray, R. and Tutu, N. K., "Intermittency and Preferential Transport of Heat in a Round Jet," *Journal of Fluid Mechanics*, Vol. 88, Sept. 1978, pp. 133–160.

[12]Antonia, R. A., Chambers, A. J., and Hussain, A. K. M. F., "Errors in Simultaneous Measurements of Temperature and Velocity in the Outer Part of a Heated Jet," *Physics of Fluids*, Vol. 23, May 1980, pp. 871–874.

[13]Goldschmidt, V. W., Moallemi, M. K., and Oler, J. W., "Structures and Flow Reversal in Turbulent Plane Jets," *Physics of Fluids*, Vol. 26, Feb. 1983, pp. 428–432.

[14]Chua, L. P. and Antonia, R. A., "The Turbulent Interaction Region of a Circular Jet," *International Communications on Heat Mass Transfer*, Vol. 13, Sept.-Oct. 1986, pp. 545–558.

[15]Browne, L. W. B., Antonia, R. A., and Chua, L. P., "Velocity Vector Cone Angle in Turbulent Flows," *Experiments in Fluids*, (to be published).

[16]Antonia, R. A., Browne, L. W. B., and Chambers, A. J., "Determination of Time Constants of Cold Wires," *Review of Scientific Instruments*, Vol. 52, Sept. 1981, pp. 1382–1385.

[17]Browne, L. W. B., Antonia, R. A., and Chua, L. P., "Calibration of X-Wires for Turbulent Flow Measurements," *Experiments in Fluids*, Vol. 7, No. 3, 1989, pp. 201–208.

[18]Lueptow, R. M., Breuer, K. S., and Haritonidis, J. H., "Computer-Aided Calibration of X-Probes Using a Lookup Table," *Experiments in Fluids*, Vol. 6, No. 2, 1988, pp. 115–118.

[19]Bradshaw, P., *An Introduction to Turbulence and Its Measurement*, Pergamon Press, Oxford, 1975.

[20]Kovasznay, L. S. G., Kibens, V., and Blackwelder, R. F., "Large-Scale Motion in the Intermittent Region of a Turbulent Boundary Layer," *Journal of Fluid Mechanics*, Vol. 41, April 1970, pp. 283–325.

[21]Antonia, R. A., "Conditionally Sampled Measurements Near the Outer Edge of a Turbulent Boundary Layer," *Journal of Fluid Mechanics*, Vol. 56, Nov. 1972, pp. 1–18.

[22]Tso, J., Kovasznay, L. S. G., and Hussain, A. K. M. F., "Search for Large-Scale Coherent Structures in the Nearly Self-Preserving Region of a Turbulent Axisymmetric Jet," *Journal of Fluids Engineering*, Vol. 103, Dec. 1981, pp. 503–508.